

30 October 1996

Landau–Pomeranchuk–Migdal effect for finite-size targets

B. G. Zakharov

*Institut für Kernphysik, Forschungszentrum Jülich,**D-52425 Jülich, Germany**L. D. Landau Institute for Theoretical Physics, GSP-1, 117940,**ul. Kosygina 2, 117334 Moscow, Russia*

Abstract

A rigorous evaluation of the Landau-Pomeranchuk-Migdal effect for finite-size targets is performed within the path integral approach previously developed in ref. [4]. The bremsstrahlung rate in QED is expressed through a solution of a two-dimensional Schrödinger equation with an imaginary potential. The boundary condition for this solution is formulated in terms of a product of the light-cone electron–photon wave function and the dipole cross section for scattering of e^+e^- pair off an atom. Numerical calculations are performed for homogeneous and structured targets. Our predictions for the homogeneous target agree well with the photon spectrum measured recently at SLAC with 25 GeV electrons. The spectra obtained for the structured two segment targets exhibit the interference minima and maxima.

1. Forty years ago Migdal [1] developed a quantum theory of suppression of the bremsstrahlung rate in a dense medium predicted by Landau and Pomeranchuk [2]. The first accurate measurement of the Landau-Pomeranchuk-Migdal (LPM) effect was recently performed at SLAC [3]. Although the experiment [3] corroborated the suppression of the radiation rate predicted in refs. [2, 1], for sufficiently thin targets the measured spectra disagree with prediction of Migdal's theory. This disagreement is presumably connected with neglecting the edge effects in ref. [1], where the case of an infinite medium was considered. Besides in ref. [1] the radiation rate for the infinite medium was calculated under certain approximations. Namely, Migdal used the Fokker-Planck approximation for evaluation of the electron density matrix. Furthermore, the inelastic processes with excitations of atoms were neglected. For these reasons Migdal's approach does not reproduce the Bethe-Heitler spectrum in a limit of low target density when the LPM suppression vanishes.

In the present paper we evaluate the LPM effect for finite-size homogeneous and structured targets within the approach developed in ref. [4]. This approach is based on the path integral treatment of multiple scattering of ref. [5], and a new formulation of the light-cone perturbation theory in terms of transverse Green's functions. Contrary to ref. [1] the approach [4] treats the evolution of the electron density matrix rigorously, and allows inclusion of inelastic processes. Within the normalization factor ~ 0.93 our results agree well with the experimental data [3] obtained for 25 GeV electron beam interacting with a homogeneous gold target. For structured targets we predict interference minima and maxima in the photon spectra.

2. In ref. [4] we reduced evaluation of the bremsstrahlung rate to solving a two-dimensional Schrödinger equation in the impact parameter space, for which the longitudinal coordinate z plays the role of time and the Hamiltonian reads

$$H = \frac{\mathbf{p}^2}{2\mu(x)} + v(\boldsymbol{\rho}, z), \quad (1)$$

Here $v(\boldsymbol{\rho}, z) = -in(z)\sigma(\rho x)/2$, $\mu(x) = E_e x(1-x)$, where $\sigma(\rho)$ is the dipole cross section for interaction of e^+e^- pair of size ρ with an atom, $n(z)$ is the target density, which is

assumed to be independent of the transverse coordinate $\boldsymbol{\rho}$, E_e is the incident electron energy, $x = k/P_e$ is the Feynman variable for the radiated photon. The probability of photon radiation obtained in ref. [4] is given by

$$\frac{dP}{dx} = 2\text{Re} \int_{-\infty}^{\infty} d\xi_1 \int_{\xi_1}^{\infty} d\xi_2 \exp \left[-\frac{i(\xi_2 - \xi_1)}{l_f} \right] g(\xi_1, \xi_2, x) [K(0, \xi_2|0, \xi_1) - K_v(0, \xi_2|0, \xi_1)], \quad (2)$$

where K is the Green's function for the Hamiltonian (1), K_v is the vacuum Green's function, $l_f = 2E_e(1-x)/m_e^2x$ is the so called photon formation length. The vertex operator $g(\xi_1, \xi_2, x)$, accumulating spin effects in the transitions $e \rightarrow e'\gamma \rightarrow e$, is given by

$$g(\xi_1, \xi_2, x) = \Lambda_{nf}(x) \frac{\mathbf{P}(\xi_2) \cdot \mathbf{P}(\xi_1)}{\mu^2(x)} + \Lambda_{sf}(x), \quad (3)$$

where $\Lambda_{nf}(x) = \alpha[4 - 4x + 2x^2]/4x$, $\Lambda_{sf}(x) = \alpha m_e^2 x [2E_e^2(1-x)^2]^{-1}$. The two terms in (3) correspond to the transitions conserving (nf) and changing (sf) the electron helicity.

For numerical evaluation of the radiation rate it is convenient to rewrite Eq. (2) in another form. Expanding K in a series in the potential v

$$K(\boldsymbol{\rho}_2, z_2|\boldsymbol{\rho}_1, z_1) = K_v(\boldsymbol{\rho}_2, z_2|\boldsymbol{\rho}_1, z_1) + \int_{z_1}^{z_2} dz \int d\boldsymbol{\rho} K_v(\boldsymbol{\rho}_2, z_2|\boldsymbol{\rho}, z) v(\boldsymbol{\rho}, z) K_v(\boldsymbol{\rho}, z|\boldsymbol{\rho}_1, z_1) + \dots,$$

after a simple algebra one can represent (2) in the form

$$\frac{dP}{dx} = \frac{dP_{BH}}{dx} + \frac{dP_{abs}}{dx}, \quad (4)$$

where

$$\begin{aligned} \frac{dP_{BH}}{dx} = & -T \cdot \text{Re} \int d\boldsymbol{\rho} \int_{-\infty}^0 d\xi_1 \int_0^{\infty} d\xi_2 g(\xi_1, \xi_2, x) K_v(0, \xi_2|\boldsymbol{\rho}, 0) \\ & \times \sigma(\rho x) K_v(\boldsymbol{\rho}, 0|0, \xi_1) \exp \left[-\frac{i(\xi_2 - \xi_1)}{l_f} \right], \end{aligned} \quad (5)$$

$$\begin{aligned} \frac{dP_{abs}}{dx} = & \frac{1}{2} \text{Re} \int_0^L dz_1 n(z_1) \int_{z_1}^L dz_2 n(z_2) \int d\boldsymbol{\rho}_1 d\boldsymbol{\rho}_2 \int_{-\infty}^0 d\xi_1 \int_0^{\infty} d\xi_2 g(\xi_1, \xi_2, x) K_v(0, \xi_2|\boldsymbol{\rho}_2, z_2) \\ & \times \sigma(\rho_2 x) K(\boldsymbol{\rho}_2, z_2|\boldsymbol{\rho}_1, z_1) \sigma(\rho_1 x) K_v(\boldsymbol{\rho}_1, z_1|0, \xi_1) \exp \left[-\frac{i(\xi_2 - \xi_1 + z_2 - z_1)}{l_f} \right]. \end{aligned} \quad (6)$$

Here $T = \int_0^L dz n(z)$ is the optical thickness of the target (we assume that $n(z) = 0$ at $z < 0$ and $z > L$). The integrals over $\xi_{1,2}$ in (5), (6) of the products of the vacuum Green's functions and exponential phase factors can be expressed through the light-cone wave function $\Psi(x, \boldsymbol{\rho}, \lambda_e, \lambda_{e'}, \lambda_\gamma)$ for the transition $e \rightarrow e'\gamma$. At $\lambda_{e'} = \lambda_e$ it is

$$\begin{aligned} \Psi(x, \boldsymbol{\rho}, \lambda_e, \lambda_{e'}, \lambda_\gamma) &= \frac{-i}{2\mu(x)} \sqrt{\frac{\alpha}{2x}} [\lambda_\gamma(2-x) + 2\lambda_e x] \left(\frac{\partial}{\partial \rho_x} - i\lambda_\gamma \frac{\partial}{\partial \rho_y} \right) \int_{-\infty}^0 d\xi K_v(\boldsymbol{\rho}, 0|0, \xi) \\ &\times \exp\left(\frac{i\xi}{l_f}\right) = \frac{1}{2\pi} \sqrt{\frac{\alpha x}{2}} [\lambda_\gamma(2-x) + 2\lambda_e x] \exp(-i\lambda_\gamma \varphi) m_e K_1(\rho m_e x), \end{aligned} \quad (7)$$

for $\lambda_{e'} = -\lambda_e$ the only nonzero component is the one with $\lambda_\gamma = 2\lambda_e$

$$\Psi(x, \boldsymbol{\rho}, \lambda_e, -\lambda_e, 2\lambda_e) = \frac{\sqrt{2\alpha x^3}}{2\mu(x)} \int_{-\infty}^0 d\xi K_v(\boldsymbol{\rho}, 0|0, \xi) \exp\left(\frac{i\xi}{l_f}\right) = \frac{-i}{2\pi} \sqrt{2\alpha x^3} m_e K_0(\rho m_e x). \quad (8)$$

Here $\alpha = 1/137$, K_0 and K_1 are the Bessel functions.

Making use of Eqs. (7), (8) one can rewrite (5), (6) in the form

$$\frac{dP_{BH}}{dx} = \frac{T}{2} \sum_{\{\lambda_i\}} \int d\boldsymbol{\rho} |\Psi(x, \boldsymbol{\rho}, \{\lambda_i\})|^2 \sigma(\rho x), \quad (9)$$

$$\begin{aligned} \frac{dP_{abs}}{dx} &= -\frac{1}{4} \text{Re} \sum_{\{\lambda_i\}} \int_0^L dz_1 n(z_1) \int_{z_1}^L dz_2 n(z_2) \int d\boldsymbol{\rho} \Psi^*(x, \boldsymbol{\rho}, \{\lambda_i\}) \\ &\times \sigma(\rho x) \Phi(x, \boldsymbol{\rho}, \{\lambda_i\}, z_1, z_2) \exp\left[-\frac{i(z_2 - z_1)}{l_f}\right], \end{aligned} \quad (10)$$

where

$$\Phi(x, \boldsymbol{\rho}, \{\lambda_i\}, z_1, z_2) = \int d\boldsymbol{\rho}' K(\boldsymbol{\rho}, z_2 | \boldsymbol{\rho}', z_1) \Psi(x, \boldsymbol{\rho}', \{\lambda_i\}) \sigma(\rho' x) \quad (11)$$

is the solution of the Schrödinger equation with the boundary condition $\Phi(x, \boldsymbol{\rho}, \{\lambda_i\}, z_1, z_1) = \Psi(x, \boldsymbol{\rho}, \{\lambda_i\}) \sigma(\rho x)$.

In ref. [6] it was shown that the p_\perp -integrated cross section for a process $a \rightarrow bc$ can be written as

$$\frac{d\sigma(a \rightarrow cb)}{dx} = \int d\boldsymbol{\rho} W_a^{bc}(x, \boldsymbol{\rho}) \sigma_{\bar{a}bc}(\rho), \quad (12)$$

where W_a^{bc} is the light-cone probability distribution for transition $a \rightarrow bc$, $\sigma_{\bar{a}bc}$ is the total cross section of interaction with the target of $\bar{a}bc$ system. For the transition $e \rightarrow e'\gamma$

the corresponding three-body cross section equals $\sigma(\rho x)$. Thus, we see that the first term in (4) equals the Bethe-Heitler cross section times the target optical thickness, *i.e.* it corresponds to the impulse approximation, while the second term describes the LPM suppression. It is worth noting that at $l_f \gg L$ the whole radiation rate can be also represented in the form analogous to Eq. (12). Indeed, in this limit the transverse variable $\boldsymbol{\rho}$ is approximately frozen, and the Green's function can be written in the eikonal form

$$K(\boldsymbol{\rho}_2, z_2 | \boldsymbol{\rho}_1, z_1) \approx \delta(\boldsymbol{\rho}_2 - \boldsymbol{\rho}_1) \exp \left[-\frac{T\sigma(\rho_1 x)}{2} \right]. \quad (13)$$

Making use of (13) we obtain in the frozen-size approximation

$$\frac{dP_{fr}}{dx} = 2 \int d\boldsymbol{\rho} W_e^{e\gamma}(x, \boldsymbol{\rho}) \left\{ 1 - \exp \left[-\frac{T\sigma(\rho x)}{2} \right] \right\}. \quad (14)$$

Eq. (14) is analogous to the formula for the cross section of heavy quark production in hadron nucleus collision obtained in ref. [6]. In QED the LPM effect at $l_f \gg L$ was previously discussed within soft photon approximation in ref. [7].

3. The dominating values of ρ in (9) are $\sim 1/m_e$. For (10) they are even smaller due to the absorption effects. For this reason the bremsstrahlung rate is sensitive only to the behavior of $\sigma(\rho)$ at $\rho \lesssim 1/m_e \ll r_B$, where r_B is the Bohr radius. We write the dipole cross section in the form

$$\sigma(\rho) = \rho^2 C(\rho), \quad (15)$$

where $C(\rho) = Z^2 C_{el}(\rho) + Z C_{in}(\rho)$. Here the terms $\propto Z^2$ and $\propto Z$ correspond to elastic and inelastic intermediate states in interaction of e^+e^- pair with an atom. For the atomic potential $\phi(r) = 4\pi(Z\alpha/r) \exp(-a/r)$ $C_{el}(\rho)$ is given by [5]

$$C_{el}(\rho) = 8\pi \left(\frac{\alpha a}{\rho} \right)^2 \left[1 - \frac{\rho}{a} K_1 \left(\frac{\rho}{a} \right) \right] \approx 4\pi\alpha^2 \left[\log \left(\frac{2a}{\rho} \right) + \frac{(1-2\gamma)}{2} \right], \quad \gamma = 0.577. \quad (16)$$

For nuclei of finite radius R_A $C_{el}(\rho \lesssim R_A) = C_{el}(R_A)$. At $\rho \ll r_B$ the factor $C_{in}(\rho)$ also can be parametrized in form (16). We use the parameters $a = 0.83 r_B Z^{-1/3}$ for the elastic component, and $a = 5.2 r_B Z^{-2/3}$ for the inelastic one. This choice allows to reproduce the elastic and inelastic contributions to the Bethe-Heitler cross section evaluated in the standard approach with realistic atomic form factors [8].

4. In Fig. 1 we compare the results of calculations (solid curve) of the bremsstrahlung rate with the one measured in [3] for a gold target with $L = 0.7\%X_0 \approx 0.023$ mm (X_0 is the radiation length) and 25 GeV electron beam. We also show the prediction of frozen-size approximation (14) (dashed curve), the radiation rate obtained for the infinite medium (long-dashed curve), and the Bethe-Heitler spectrum (dot-dashed curve). We have found that the normalization of the experimental spectrum disagrees with our theoretical prediction. The theoretical curves in Fig. 1 were multiplied by the factor 0.93. This renormalization brings the calculated spectrum in a good agreement with the data of ref. [3]. The origin of the above disagreement in normalization is not clear. The authors of ref. [3] give the systematic error 3.2%. However, normalizations of the spectrum for gold targets with $L = 0.7\%X_0$ and $L = 0.1\%X_0$ at the photon momentum $k \sim 500$ MeV, where the LPM suppression is expected to be small, differ by $\sim 20 - 30\%$.

For 25 GeV electrons $l_f \approx 0.47 \cdot (1\text{MeV}/k(\text{MeV}))$ mm in the region of k shown in Fig. 1. One can conclude from this figure that the radiation rate calculated using Eqs. (4), (9), (10) is close to the prediction of the frozen-size approximation (14) for the photons with $l_f \gtrsim L$, while for the photons with $l_f \lesssim L$ it is close to the spectrum for the infinite medium. To illustrate the role of the finite target thickness better we present in Fig. 2 the LPM suppression factor defined as $S = dP/dx/dP_{BH}/dx$ as a function of the ratio $h = L/l_f$ for several values of the photon momentum. The calculations were performed for a gold target and 25 GeV electron beam. Fig. 2 demonstrates that the edge effects come into play at $L \lesssim l_f$. One can also see from Fig. 2 that for low photon momenta the edge effects vanish faster. This fact is a consequence of a stronger suppression of the coherence length in radiation of soft photons.

Notice that the suppression factor has a minimum at $L \approx l_f$ for 100 and 400 MeV photons. This minimum reflects the two-edge interference for a plate target. One can expect a more pronounced interference effects for structured targets. In Fig. 3 we show our results for the LPM suppression factor for a two segment gold target. Qualitatively our results for the interference effects are similar to those of ref. [9], in which

the bremsstrahlung rate for structured targets was evaluated modelling the medium by the potential $U(\boldsymbol{\rho}, z) = -\boldsymbol{\rho} \cdot \mathbf{E}_\perp(z)$, where \mathbf{E}_\perp is a random transverse electric field [10]. However, for our realistic electron-atom interaction the maxima and minima in the spectra are less pronounced than for the model medium used in ref.[9]. For a homogeneous target our spectrum differs from obtained by Blankenbecler by $\sim 10\%$.

The reason for this disagreement is as follows. Using the technique of refs. [5, 4] one can show that the model potential of refs. [10, 9] translates in our approach to the following choice of the dipole cross section

$$\sigma(\rho) = \frac{2\pi\alpha\rho^2}{n} \int_{-\infty}^{\infty} dz \langle \mathbf{E}_\perp(0) \cdot \mathbf{E}_\perp(z) \rangle$$

in which the important logarithmic ρ -dependence which derives from the Coulomb interaction is missed. We conclude that the model of refs. [10, 9] is too crude for a quantitative simulation of the LPM effect in a real medium.

To summarize, we evaluated the LPM effect in QED for finite-size homogeneous and structured targets. For the first time we performed a rigorous theoretical analysis of the experimental data on the LPM effect obtained at SLAC [3]. The theoretical predictions up to a normalization factor 0.93 are in a good agreement with the spectrum measured at SLAC [3] for the homogeneous gold target with $L = 0.7\%X_0$ and 25 GeV electron beam. For structured targets we predict minima and maxima in the photon spectra.

I would like to thank B.Z. Kopeliovich and N.N. Nikolaev for discussions and reading the manuscript. I am grateful to J. Speth for the hospitality at KFA, Jülich, where a part of this work was done.

References

- [1] A.B. Migdal, Phys. Rev. **103** (1956) 1811.
- [2] L.D. Landau and I.Ya. Pomeranchuk, *Dokl. Akad. Nauk SSSR* **92** (1953) 535, 735.
- [3] P.L. Anthony, R. Becker-Szendy, P.E. Bosted *et al.*, Phys. Rev. Lett. **75** (1995) 1949.
- [4] B.G. Zakharov, JETP Lett. **63** (1996) 952.
- [5] B.G. Zakharov, Sov. J. Nucl. Phys. **46** (1987) 92.
- [6] N.N. Nikolaev, G.Piller and B.G. Zakharov, JETP **81** (1995) 851.
- [7] N.F.Shul'ga and S.P. Fomin, JETP Lett. **63** (1996) 873.
- [8] Y.-S. Tsai, Rev. Mod. Phys. **46** (1974) 815.
- [9] R. Blankenbecler, Preprint SLAC-PUB-96-7156, Stanford, 1996.
- [10] R. Blankenbecler and S.D. Drell, Phys. Rev., **D53** (1996) 6265.

Figures:

Figure 1: The bremsstrahlung spectrum for 25 GeV electrons incident on a gold target with a thickness of $0.7\%X_0$. The experimental data are from ref. [3]. The full curve shows our results obtained using Eqs. (9), (10). The dashed curve was obtained in the frozen-size approximation (14). The long-dashed curve shows the spectrum for the infinite medium. The Bethe-Heitler spectrum is shown by the dot-dashed curve.

Figure 2: The LPM suppression factor for 25 GeV electron incident on a homogeneous gold target as a function of the ratio $h = L/l_f$ and the photon momentum.

Figure 3: The LPM suppression factor for 25 GeV electron incident on a two segment gold target. The thickness of each segment is $0.35\%X_0$. The set of gaps is as follows: 0 (solid curve), $0.7\%X_0$ (dotted curve), $1.4\%X_0$ (dashed curve), $2.1\%X_0$ (long-dashed curve), $3.5\%X_0$ (dot-dashed curve).

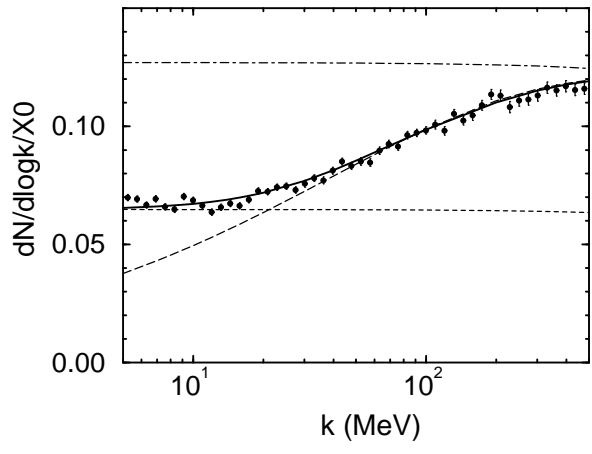


Fig.1

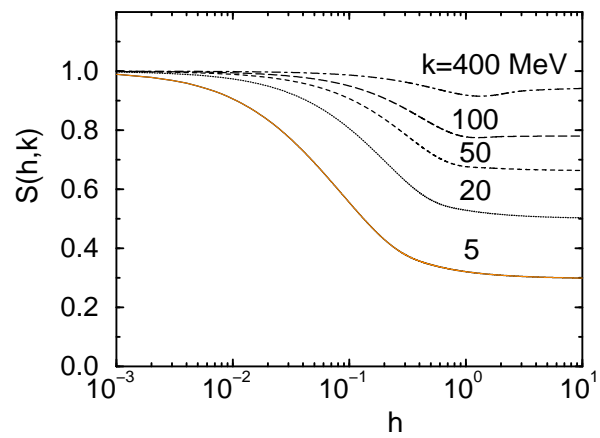


Fig. 2

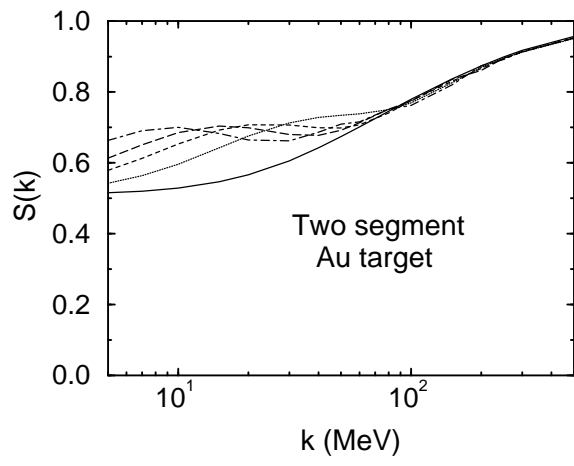


Fig. 3